THE ASTROPHYSICAL JOURNAL, 456:217–224, 1996 January 1

CN ZEEMAN OBSERVATIONS OF MOLECULAR CLOUD CORES

RICHARD M. CRUTCHER,[1] THOMAS H. TROLAND,[2] BERNARD LAZAREFF,[3] AND ILYA KAZÈS[4]

Received 1995 April 10; accepted 1995 July 6

ABSTRACT

We present results from the first attempt to measure strengths of magnetic fields in dense molecular cloud cores by observations of the Zeeman effect in the 3 mm lines of CN. The observations were made with the 30 m IRAM radio telescope with a new polarimeter constructed for this experiment. The two molecular cores which were observed are located about 3′ north of Orion-KL (OMC-N4) and about 1′ east of IRS 4 in S106 (S106-CN). From CN data for OMC-N4 and S106-CN, respectively, we estimate cloud radii of 0.03 and 0.05 pc, masses of 10 and 22 $M_\odot$, and H_2 densities of 1.6×10^6 cm^{-3}. Our CN Zeeman results for the line-of-sight magnetic fields are B_{los}(OMC-N4) $= +79 \pm 99$ μG and B_{los}(S106-CN) $= -57 \pm 199$ μG. Hence, we did not detect magnetic fields. Our upper limits for B_{los} are significantly less than field strengths expected for assumption of internal motions at the Alfvén speed, of a critical mass to magnetic flux ratio, or of virial equilibrium, but the very small sample of clouds and the uncertainties in the $|\boldsymbol{B}|_{\rm Alfvén}$, $|\boldsymbol{B}|_{\rm critical}$, and $|\boldsymbol{B}|_{\rm virial}$ estimates preclude definite conclusions.

Subject headings: ISM: clouds — ISM: magnetic fields — ISM: molecules — polarization

1. INTRODUCTION

Understanding the physics governing the structure and evolution of dense interstellar clouds is a necessary step toward understanding the fundamental astrophysical process of star formation. In the past decade it has become increasing clear that this physics cannot be understood in the absence of magnetic fields. This conclusion is based in part upon the need to support dense clouds against self-gravity and upon the deficiencies of other proposed mechanisms to do so. The crucial parameter characterizing magnetic support is the ratio of mass to magnetic flux in a cloud, M/Φ_B. If this ratio is less than a critical value $(M/\Phi_B)_{\rm critical} \approx 0.13$ G$^{-1/2}$ (Mouschovias & Spitzer 1976), the cloud is said to be *magnetically subcritical*, and static magnetic fields support it perpendicular to the field direction irrespective of external pressure. Otherwise, the cloud is *magnetically supercritical*, and it cannot be supported by static magnetic field pressure alone. Even in this latter case, however, magnetic fields may indirectly provide additional support in the form of kinetic energy in magnetohydrodynamical waves. The ratio M/Φ_B is directly proportional to the observable ratio $N/|\boldsymbol{B}|$. Hence, observations of column densities and magnetic field strengths in dense cloud cores are crucial to our understanding of star formation.

The only currently viable technique for measuring the strengths of magnetic fields in interstellar clouds is to detect the Zeeman effect in spectral lines arising in the clouds. If the spectral line-forming region is permeated by a field $\boldsymbol{B}$, the normal Zeeman effect splits a line with rest frequency ν_0 into three separate polarized components with frequencies ν_0-ν_z, ν_0, and $\nu_0 + \nu_z$, where $2\nu_z = |\boldsymbol{B}|Z$. The Zeeman factor Z (in Hz μG^{-1}) is 2.80 for the 1420 MHz H I line, and it is 3.27 and 1.96 for the 1665 and 1667 MHz OH lines, respectively. Other paramagnetic molecules such as CN, CCS, and SO (but unfortunately not CO) have Z values approximately equal to those for H I and OH. Although in principle it is possible to determine the complete orientation and magnitude of $\boldsymbol{B}$ from Zeeman observations, in practice sensitivity limits us to measurement of the line-of-sight component $B_{los} = |\boldsymbol{B}| \cos\theta$, where θ is the angle between the line of sight and the magnetic field (Crutcher et al. 1993). We measure B_{los} by observing the line strength T in both right (R) and left (L) circular polarization in order to determine the Stokes parameter $V \equiv T_R - T_L = +[dI/dv]v_z \cos\theta$, where the Stokes parameter $I \equiv T_R + T_L$.

Zeeman effect measurements have been made in thermally excited lines of H I and OH. Although H I Zeeman observations can be useful for molecular clouds (e.g., Roberts et al. 1993), molecular line observations are necessary to probe the denser regions. Single-dish Zeeman observations of OH ground-state lines have revealed B_{los} as high as 140 μG (see review by Troland 1990), while OH aperture synthesis observations have yielded B_{los} of 400 μG (Roberts, Crutcher, & Troland 1995). The OH Zeeman effect observations have established that $|\boldsymbol{B}|/N$(H) is high enough in some clouds to provide magnetic support (Crutcher 1988; Troland 1990; Crutcher et al. 1993; Roberts et al. 1995), and a detailed comparison between observations and a theoretical model of a magnetically supported cloud (Crutcher et al. 1994) has provided support for the theory. However, while valuable, these results may apply only to magnetic fields in regions of intermediate density [typically $n(H_2) \approx 10^{3-4}$ cm^{-3}]. In general, [OH/H_2] decreases significantly at higher densities (Troland et al. 1995), making OH a poor probe of magnetic fields in dense cloud cores. Yet the most crucial aspects of star formation (e.g., the onset of core collapse, the dispersal of angular momentum) are predicted to occur in regions of high density. For this reason, Zeeman effect measurements sensitive to magnetic fields at $n(H_2) > 10^4$ cm^{-3} are essential. In this paper we argue that CN Zeeman observations have the potential to probe magnetic fields in dense cores and describe the first attempt to do this.

[1] Department of Astronomy, University of Illinois, Urbana, IL 61801.
[2] Department of Physics and Astronomy, University of Kentucky, Lexington, KY 40506.
[3] IRAM, 300, Rue de la Piscine, Domaine Universitaire, 38406 St-Martin-D'Heres, France.
[4] Observatoire de Paris-Section de Meudon, Place Jules Janssen, F-92195 Meudon, France.

2. THE CN ZEEMAN EFFECT

We believe that CN offers the best opportunity to measure magnetic fields in clouds with densities of 10^{5-6} cm^{-3}. The critical density at which the collisional excitation rate equals the Einstein A-value is $n(H_2) \approx 10^5$ cm^{-3} for the $N = 1 \rightarrow 0$ transition of CN ($A_{10} = 1.2 \times 10^{-5}$ s^{-1}). The CN ground state is $^2\Sigma$; and the $N = 1 \rightarrow 0$ transition has a total of nine hyperfine components, of which seven are strong. In Table 1 we list relevant information about these seven transitions, including the relative line intensity (R.I.) and line frequency, our calculated Zeeman splitting factor Z (in Hz μG^{-1}), and the relative sensitivity of each transition to the Zeeman effect ($Z \times$ R.I.). We calculated the Z value for each transition from the molecular g-factor given in § 11.8b of Gordy & Cook (1984), taking into account the hyperfine structure of CN as explained in § 11.2a. This is the procedure followed by Bel & Leroy (1989), who published Z for only two of the seven transitions.

The existence of seven hyperfine lines is highly favorable for CN Zeeman observations. The different Z values of the transitions (including one with reversed sign) permit a distinction to be made between the Zeeman effect and instrumental effects such as those arising from telescope "beam squint." Beam squint amounts to a small offset of the telescope beam in opposite senses of circular polarization. If a velocity gradient exists in the source, beam squint can create a residual curve in the Stokes V spectrum identical to that of the Zeeman effect. Another possible spurious effect can be produced by imperfect Doppler tracking and nonsimultaneous observations of the L and R circularly polarized lines. However, the sign and amplitude of the Stokes V signal produced by both of these instrumental effects are the same for all hyperfine transitions, while the sign and amplitude of the Zeeman contributions to the Stokes V spectrum are multiplied by the different Z factors of Table 1. In order to separate the spurious and Zeeman signals, our analysis procedure consisted of a least-squares fit in frequency v, simultaneously to all seven of the hyperfine line V spectra, of the function

$$V_i(v) = C_1 I_i(v) + C_2[dI_i(v)/dv] + C_3 Z_i[dI_i(v)/dv], \quad i = 1, 7. \tag{1}$$

In this expression, $V_i(v)$ and $I_i(v)$ are the Stokes V and I spectra for each of the seven hyperfine CN lines. The results of the fit are C_1, a measure of the gain difference in the telescope between R and L circular polarizations, C_2, a measure of any instrumental effects that produce a spurious frequency shift between the R and L circularly polarized lines, and $C_3 = B_{los}/2$. The procedure of equation (1) is the same as that of Crutcher et al. (1993), except that the simultaneous fitting to seven CN lines with different Z's permitted a distinction to be made between C_2 and C_3.

In order to test how well our fitting procedure separated the contributions to the V spectra produced by magnetic fields and instrumental effects, we carried out numerical tests. We constructed Gaussian CN lines with optically thin LTE intensities and superposed a random channel-to-channel noise on the spectra. We then put in a line-of-sight magnetic field and beam squint/velocity gradient effects. The magnetic field strength corresponded to $B_{los} = 2\,\sigma$, where σ was the error reported by the least-squares routine in B_{los} due to the random channel-to-channel noise we introduced. We imposed a velocity gradient/beam squint effect on the synthetic V spectra such that C_2/C_3 ranged from 0 to 4; i.e., for the range of no instrumental effect to the contribution due to B_{los} being dominated by instrumental effects. Our least-squares fitting procedure always recovered the correct C_2 and C_3 within 1 σ, independent of C_2/C_3. Moreover, a large instrumental effect did not significantly increase the error in the determination of B_{los}. We also made 20 computer runs with σ of the channel noise always the same but with different random noise patterns; B_{los} was found to differ slightly from run to run, but always within 1 σ of the correct value. In addition, $\sigma(B_{los})$ determined from the scatter in the 20 separate determinations with differing noise patterns agreed with $\sigma(B_{los})$ determined by the least-squares procedure for a single run. We conclude that the procedure works correctly and that instrumental effects produced by beam squint and velocity gradients can be separately and accurately determined without significantly reducing our sensitivity to B_{los}.

A crucial question is whether we can achieve the sensitivity necessary to detect fields at the level predicted theoretically for the $n(H_2) \sim 10^6$ cm^{-3} cores of star-forming clouds. If a single receiver system is used, so that one observes only one circular polarization at a time, it is straightforward to show that for a Gaussian line shape the 1 σ sensitivity to B_{los} is $\sigma_B \approx 2Z^{-1}[T_{sys}/T_{line}]\,[\Delta v/t]^{1/2}$, where T_{sys} is the system noise temperature, T_{line} is the peak intensity of the Gaussian line, Δv is the full-width at half-maximum of the Gaussian (in frequency units), and t is the observing time. For the case of CN, if all seven transitions in Table 1 are observed simultaneously and they are in the given relative intensity ratios, σ_B(seven lines) $\approx 0.43\sigma_B(F = 5/2 \rightarrow 3/2)$; then $\sigma_B \approx 16[T_{sys}/T_{line}]\,[\Delta V\ (\text{km s}^{-1})/t(\text{hr})]^{1/2}$ μG. These expressions are in reasonable agreement with our extensive experience in OH and H I Zeeman observations and with the CN Zeeman observations reported here. Hence, we can achieve $\sigma_B \approx 120$ μG for $T_{sys} \approx 300$ K, $T_{line} \approx 10$ K, $\Delta V \approx 2$ km s^{-1}, and $t \approx 30$ hr, which is sufficient sensitivity to measure the expected fields in the dense star-forming cores of clouds.

TABLE 1

ZEEMAN SPLITTINGS FOR CN $N = 1 \rightarrow 0$

Number: $(N', J', F') \rightarrow (N, J, F)$	R.I.	ν_0(GHz)	Z(Hz μG^{-1})	$Z \times$ R.I.
1. (1, 1/2, 1/2) → (0, 1/2, 3/2).....	8	113.14434	2.18	17.4
2. (1, 1/2, 3/2) → (0, 1/2, 1/2).....	8	17087	−0.31	2.5
3. (1, 1/2, 3/2) → (0, 1/2, 3/2).....	10	19133	0.62	6.2
4. (1, 3/2, 3/2) → (0, 1/2, 1/2).....	10	48839	2.18	21.8
5. (1, 3/2, 5/2) → (0, 1/2, 3/2).....	27	49115	0.56	15.1
6. (1, 3/2, 1/2) → (0, 1/2, 1/2).....	8	49972	0.62	5.0
7. (1, 3/2, 3/2) → (0, 1/2, 3/2).....	8	50906	1.62	13.0

3. OBSERVATIONS

3.1. *IRAM* 30 m *Telescope and Polarimeter*

Because the sensitivity of Zeeman-effect measurements of magnetic field strengths is directly proportional to the line strength, and because the dense cores we plan to study are quite small, it is highly advantageous to use the largest possible telescope. Our CN Zeeman-effect observations were therefore made with the 30 m IRAM telescope, which has a full width at half-power beam diameter of 23″ at 113 GHz. The receiver had a single-channel SIS mixer which detected linear polarization. A polarimeter was constructed to convert circular polarization from the sky to linear polarization and to switch between senses of circular polarization. The polarimeter consisted of a $\lambda/4$ transmission plate which could be rotated between position angles $\pm 45°$ in order alternately to measure the two senses of circular polarization. The polarimeter was installed in front of the dichroic frequency splitter normally used at the 30 m telescope to allow simultaneous observations at 2.6 mm and 1.3 mm wavelengths; the frequency splitter had its wire grid removed, so that it was in effect a plane mirror. The electronic drive circuit of the polarimeter featured a phase time adjustable between approximately 1 and 2 s. The dead time during which the plate was moving between two position was approximately 0.25 s. The polarimeter electronics sent blanking and status signals to the receiver room; the telescope control software was modified so that the polarimeter signals were used to control the spectrometer.

Initial installation, testing, and commissioning of the polarimeter at the 30 m telescope took place 1994 February 23–25. An important instrumental effect when using a polarimeter to measure Zeeman line shifts in astronomical sources is the beam squint. Because of small asymmetries in the illumination or in the telescope optics, the R and L polarized beams of a telescope may point to slightly different directions and/or have different shapes. In the presence of velocity gradients, this introduces a frequency shift between the R and L spectral lines which can masquerade as a Zeeman signal. Our analysis procedure for the CN data (§ 2) allows us to eliminate these effects from the Zeeman analysis, but it is important to know just what the instrumental polarization characteristics are.

In order to study the circular polarization properties of the telescope, three types of measurements were carried out. First, the Stokes V intensity was mapped over a small unpolarized continuum source, Venus. The resulting maps (Fig. 1 shows one example) represent the polarized beam of the telescope. Because it took several minutes to make such maps and because the weather was not very stable during the times these maps were made, low-level details are not reliable. Hence, it was not possible to say whether there is a polarized beam effect other than beam squint. However, all such maps show the same two-lobed structure seen in Figure 1. Second, we made a series of four-point Stokes V maps for other planets and continuum sources, with the four points either 10″ or 15″ in the cardinal directions (with respect to the azimuth-elevation coordinate system) from source centers. These data were sufficient to derive the beam squint over extended ranges of azimuth and elevation. Finally, we used the 500 channel 1 MHz filter spectrometer to attempt to measure any dependence of beam squint on frequency; because no frequency dependent effect was seen in the 1 MHz data the spectral data were smoothed to 16 MHz in order to improve the sensitivity.

Our conclusions are that the beam squint is about 0.″25 or 1% of the Stokes I beam diameter, that it is independent of the azimuth and elevation of the telescope, and that there is a reproducible but very weak dependence of the beam squint on frequency over the 500 MHz bandpass of the telescope. Stokes V measurements which would produce a sensitivity to $B_{los} = 100\ \mu$G would be equally sensitive to a linear velocity gradient of about 1 m s^{-1} arcsec^{-1} (too small to measure directly) if that gradient were aligned with the beam squint. Since the beam squint is fixed in amplitude and position angle, the effects of beam squint on Zeeman data will be lower because of the rotation of Zeeman sources in the telescope beam as the alt-azimuthally mounted telescope tracks source positions. Based on our numerical tests (§ 2) and the small amplitude of the beam squint, we are confident that such instrumental effects can be eliminated by our Zeeman analysis procedure without affecting the sensitivity to the Zeeman effect.

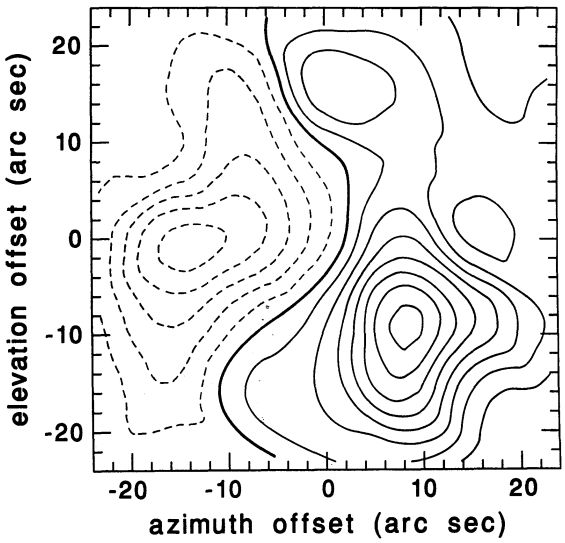

FIG. 1.—Stokes parameter V continuum map of Venus. The scale is such that Venus produces a peak signal ($I/2$) of about 21,000 units; the contour interval is 50 units, with negative contours plotted as dashed lines and the zero level plotted as a heavy solid line. The two-lobed structure which is observed is the signature of a telescope beam squint with an amplitude of about 0.″27 and a position angle of about 70°.

3.2. CN *Observations*

CN Zeeman observations took place between 1994 October 3 and September 27. In the time available only two molecular clouds could be observed. The positions observed are given in Table 2. One was a position about 3′ north of the Orion-KL molecular cloud where Turner & Thaddeus (1977) found that CN lines were extraordinarily strong. Wilson & Johnston (1989) mapped this OMC-N cloud with the VLA (12.″5 resolution) in the H_2CO 2 cm line in emission and found six high-density fragments. We made five-point maps of the CN line centered on each of their six positions in order to select our Zeeman position. The position we choose is the CN peak position in OMC-N4, which is 12″ south of the OMC-N4 H_2CO peak. The second cloud is the CN peak toward S106. Churchwell & Beiging (1982) mapped S106 in the $N = 1 \rightarrow 0$ CN line with 1′ resolution and found a CN peak about 1′ east of the central star, IRS 4. R. Simon (private communication) has mapped S106 in the $N = 1 \rightarrow 0$ and $2 \rightarrow 1$ CN lines with the IRAM 30 m telescope; we used Simon's higher angular

TABLE 2

CN ZEEMAN RESULTS

Item	OMC-N4	S106-CN
α_{1950}	$05^h32^m49\overset{s}{.}3$	$20^h25^m36\overset{s}{.}6$
δ_{1950}	$-05°21'24''$	$+37°12'56''$
R	0.03 pc	0.05 pc
ΔV	1.4 km s^{-1}	1.6 km s^{-1}
τ_5	0.92	0.56
T_{ex}	36 K	26 K
$N(CN)_{LTE}$	1.5×10^{15} cm^{-2}	0.6×10^{15} cm^{-2}
$N(H_2)_{CN}$	3.0×10^{23} cm^{-2}	1.2×10^{23} cm^{-2}
M_{virial}	10 $M_\odot$	22 $M_\odot$
$n(H_2)_{virial}$	1.6×10^6 cm^{-3}	0.7×10^6 cm^{-3}
$N(H_2)_{virial}$	1.9×10^{23} cm^{-2}	1.5×10^{23} cm^{-2}
$\|B\|_{Alfven}$	500 μG	500 μG
$\|B\|_{critical}$	1200 μG	480 μG
$\|B\|_{virial}$	830 μG	650 μG
$B_{los} \pm 1\text{-}\sigma$	$+79 \pm 99$ μG	-57 ± 199 μG

resolution maps to define the S106 CN peak position for our Zeeman observations.

In order to observe all seven CN hyperfine components simultaneously, the 30 m telescope autocorrelation spectrometer was divided into six banks. Each bank had a total bandwidth of 20 MHz (about 53 km s^{-1}) and 256 spectral channels, for a velocity resolution of about 0.2 km s^{-1}. One bank was centered between hyperfine lines no. 4 and no. 5 (see Table 1), while the others were each centered on the remaining five hyperfine lines. The average system noise temperature was about 330 K. Stokes I spectra were obtained using the normal position switched technique, with about 20 minutes on-source integration time. Stokes V spectra were obtained by polarization switching only, with about 18 hr of integration time for each cloud. Figure 2 shows all of the spectra.

3.3. CN *Zeeman Results*

Using the fitting process represented by equation (1), we derived values for C_1, C_2, and $C_3 = B_{los}/2$ for each of the two sources. For neither of the clouds was a statistically significant value for C_2 found, which implies that the combined instrumental polarization and velocity gradient effects were not important. Values derived for B_{los} are listed in Table 2; the magnetic field was not detected toward either cloud. In order to illustrate the signals in the Stokes V spectra which would be observed if a sufficiently strong magnetic field were present, Figure 2 shows dI/dv superposed on the observed V spectra for B_{los} of 5 σ (500 μG for OMC-N4 and 1000 μG for S106-CN, respectively).

3.4. CN *I Spectra Results*

Wilson & Johnston (1989) found a mean radius of 0.027 pc (18″) for OMC-N4 from the VLA 2 cm H_2CO line map. Our own (crude) map in the CN line suggests a radius of 0.03 pc, which we adopt here. Simon's CN map of S106 suggests $R \approx 0.05$ pc (17″). This value is confirmed by observations of Crutcher & Troland (unpublished) of S106-CN with the NRAO 12 m telescope. The S106-CN lines are approximately 2.8 times weaker when observed with the smaller telescope, which is the expected ratio for a CN cloud with (an assumed) Gaussian radial intensity distribution and a half-intensity radius of $\sim$17″. We list the cloud radii in Table 2.

The Stokes I spectra are reasonably consistent with LTE intensity ratios and moderate line optical depths, although there are clearly small deviations from LTE. Assuming LTE among the hyperfine levels involved in the $N = 1 \rightarrow 0$ lines, we have followed the procedure of Crutcher et al. (1984) to derive the column density of CN in the $N = 0$ and 1 states. Table 2 gives the full-width at half-maximum of the lines ΔV, the optical depth τ_5 of the strongest hyperfine line (no. 5 in Table 1), and the excitation temperature T_{ex} of the $N = 1 \rightarrow 0$ transition. Finally, we assumed LTE among the rotational levels N in order to find the total column density N(CN) in all rotational states.

4. DISCUSSION

The two high-density cloud cores we observed were chosen both because strong CN lines were present and because strong magnetic fields had previously been detected. Toward Orion A Troland, Crutcher, & Kazès (1986) found $B_{los} \approx 125$ μG in a single-antenna OH Zeeman absorption-line observation, which would spatially average any field strength variations over the entire continuum source. Troland, Heiles, & Goss (1989) found $B_{los} \approx 100$ μG in VLA H I Zeeman maps of Orion A, with an increase from $B_{los} \approx 40$ μG near the continuum peak to a maximum $B_{los} = 174 \pm 45$ μG at a position 2′ to the north. The position of this maximum B_{los} is only 1.′5 (0.2 pc) from our OMC-N4 position. Preliminary results from a higher sensitivity and angular resolution repeat of this experiment have found $B_{los} > 200$ μG. Hence, Zeeman observations of lines which trace lower densities than CN suggest that $B_{los} \gtrsim 200$ μG south of OMC-N4 with B_{los} increasing northward. Our CN results imply that $B_{los} \lesssim 300$ μG (3 σ) at the OMC-N4 position. In VLA OH Zeeman maps toward S106, Roberts et al. (1995) found $B_{los} = 400 \pm 30$ μG at a position 30″ (0.09 pc) west of S106-CN. Their maps of OH optical depth show that the molecular cloud must be centered to the east of the eastern edge of the S106 radio continuum emission. The data are consistent with the OH and CN Zeeman observations sampling the same cloud core (located just east of the S106 continuum), although at slightly different positions. Our CN results imply that $B_{los} \lesssim 600$ μG (3 σ) at the S106 CN peak position. Although our CN results for both clouds are consistent (at the 3 σ level) with the H I and OH Zeeman measurements of magnetic fields, it is surprising that there is no hint of a magnetic field in the CN Stokes V spectra.

There are three ways to estimate the "expected" magnetic field strengths toward the two molecular cores we have observed. (1) Observed line widths in molecular clouds are generally found to be supersonic. If motions are not super-Alfvénic, then an estimate of the magnetic field strength may be obtained from the observed line widths and an estimate of the density. Uncertainties are due to uncertainties in the volume density and in how the Alfvén velocity is reflected in the line width. (2) Models such as those of Mouschovias (1976) of magnetically supported clouds yield a prediction of (M/Φ_B), which can be directly related to the observable $N_H/|B|$. So an estimate of the hydrogen column density from molecular line observations leads to an estimate for the field strength. Such detailed models have included only the support provided by the static magnetic field and thermal motions and are therefore inconsistent in detail with observed cloud cores, which have superthermal motions. Hence, because the additional support of fluctuating magnetic fields has been neglected, $|B|_{critical}$ from these models would be expected to yield an overestimate of the strength of the actual static magnetic fields. (3) The virial theorem may be used, including the effects of magnetic pres-

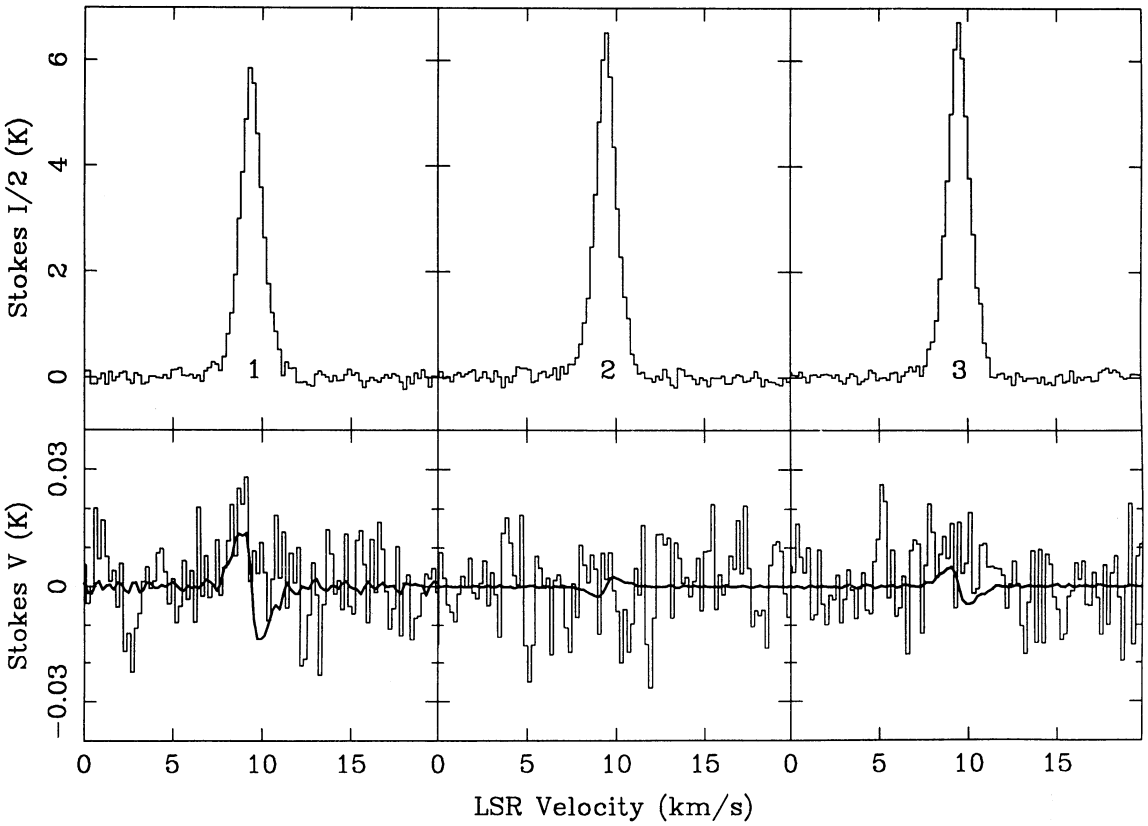

FIG. 2*a*

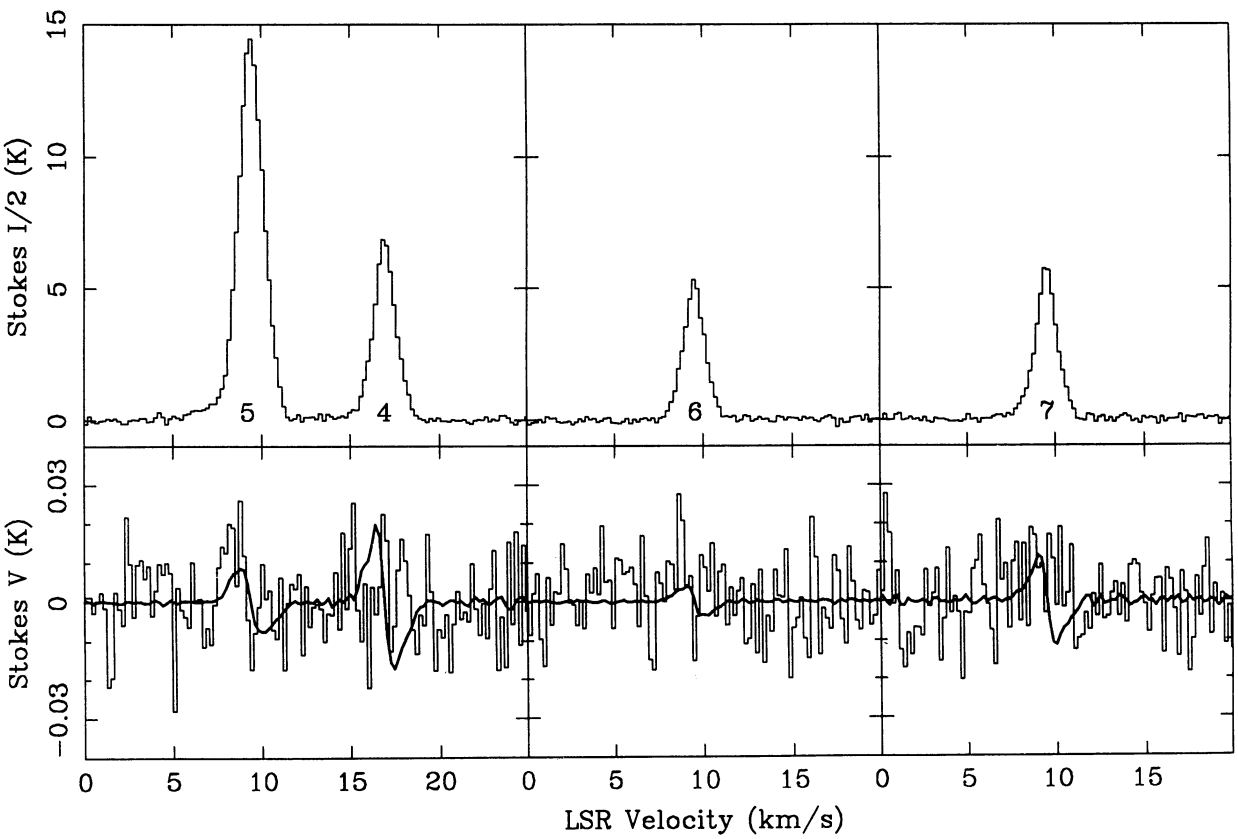

FIG. 2*b*

FIG. 2.—Stokes parameter $I/2$ (*top*) and V (*bottom*) spectra toward OMC-N4 (*a* and *b*) S106-CN (*c* and *d*) and for the seven strongest CN hyperfine components of the $N = 1 \rightarrow 0$ transition. The numbers at the zero intensity level of each I line identify the hyperfine transition in Table 1.

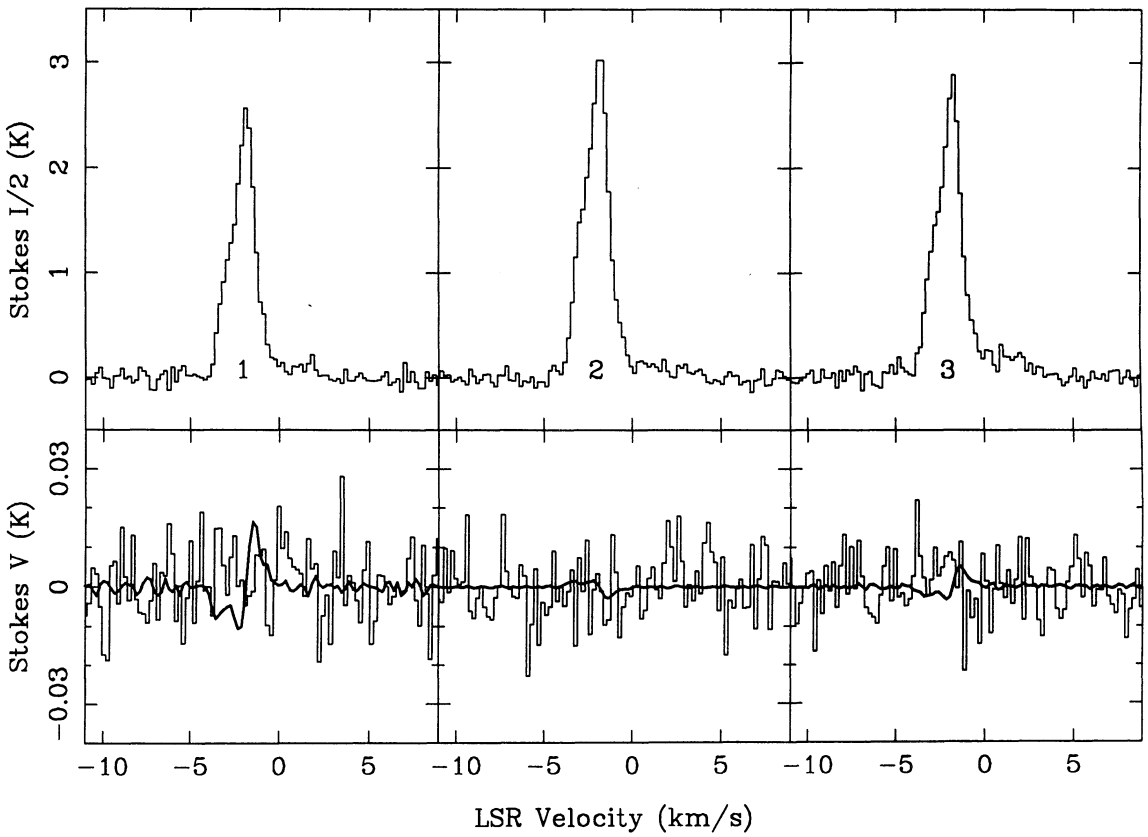

FIG. 2*c*

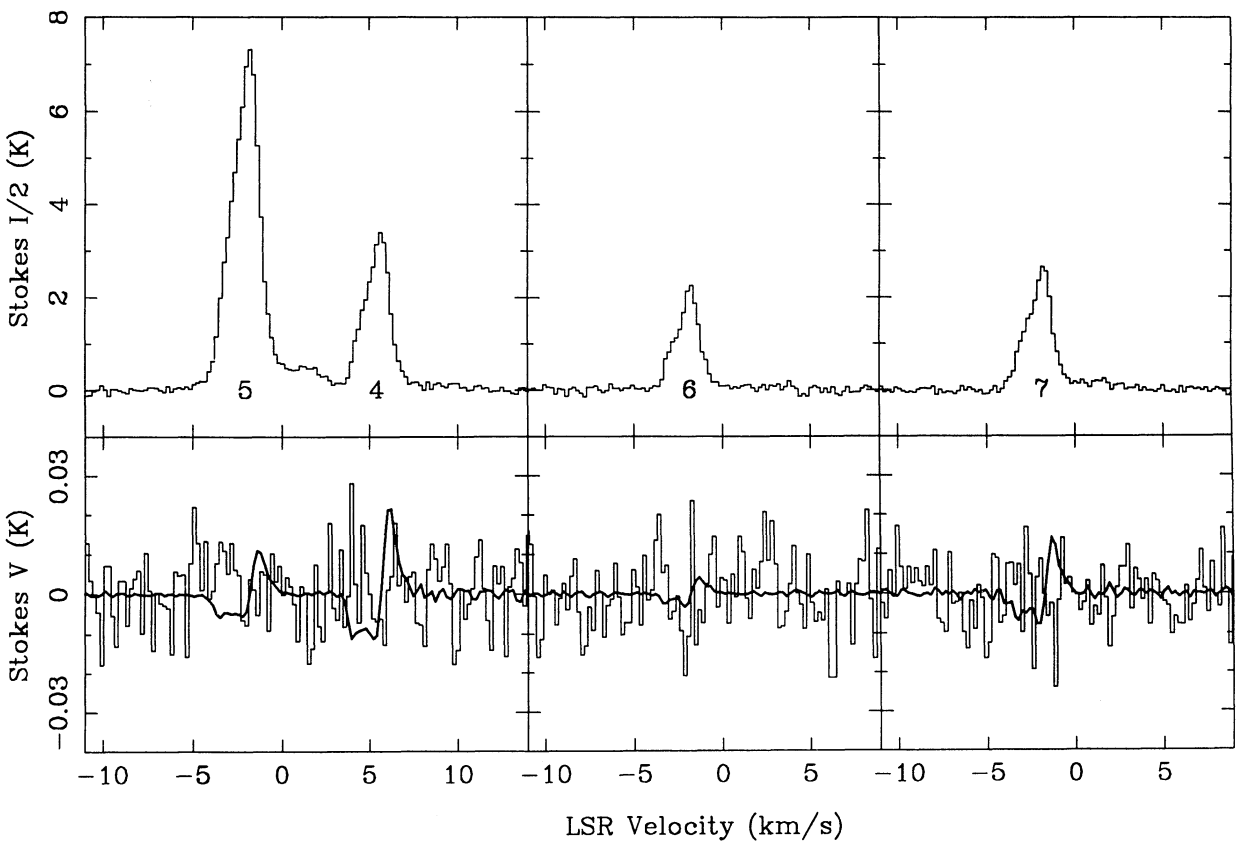

FIG. 2*d*

sure and supersonic motions (due to MHD waves), to estimate mass and magnetic field strengths of clouds.

We first estimate $|\boldsymbol{B}|$ from the Alfvén velocity. Toward both clouds $T_{ex}(CN) \approx 30$ K. Observations of ^{12}CO suggest that the kinetic temperature $T_K \approx 30$ K in the two clouds (Batrla et al. 1983; Bally & Scoville 1982). Therefore, $T_{ex}(CN) \approx T_K$; in order for the CN excitation to be thermalized by collisions, $n(H_2) \gg 10^5$ cm^{-3}, the critical density of the $N = 1 \rightarrow 0$ transition. Moreover, the thermal line width of the CN lines at $T_K = 30$ K is $\Delta V = 0.23$ km s^{-1}, which is much smaller than the observed line widths. The superthermal line widths suggest that $|\boldsymbol{B}| \gtrsim 500$ μG in order that the supersonic velocities be sub-Alfvénic for $n(H_2) \approx 10^6$ cm^{-3}.

If there were a universal $[CN/H_2]$ ratio, we could infer $N(H_2)$ from $N(CN)$ and compare our upper limits to B_{los} with $|\boldsymbol{B}|_{critical}$, which is the minimum expected value if the clouds are supported by a static magnetic field. With a mean molecular weight of 2.33, $(M/\Phi_B)_{critical} \approx 0.13$ G$^{-1/2}$ (Mouschovias & Spitzer 1976) implies

$$|\boldsymbol{B}|_{critical} \approx 8 \times 10^{-21} N(H_2)\ \mu G\ cm^{-2}\ . \quad (2)$$

Crutcher, Churchwell, & Ziurys (1984) found an average value $\log [CN/H_2] \approx -8.3$ in a study of seven positions in six dark clouds. If this relative abundance of CN is correct for OMC-N4 and S106-CN, our LTE values for $N(CN)$ yield $|\boldsymbol{B}|_{critical} \approx 1200$ and 480 μG, respectively. Unfortunately, $[CN/H_2]$ is probably highly variable; the range for the six dark clouds was $-7.3 \gtrsim \log [CN/H_2] \gtrsim -9.7$. Theoretical predictions of CN abundance depend sensitively on radiation field, gas density, metal abundance, and cloud age. Graedel et al. (1982) included CN in their study of time-dependent chemistry in molecular clouds. They found that $\log [CN/H_2] \approx -6$ in young (10^{5-6} yr old) clouds independent of cloud density and metal abundance, but after 10^8 yr $\log [CN/H_2] < -10$ for $n(H_2) > 10^5$ cm^{-3}. Thus, $|\boldsymbol{B}|_{critical}$ is uncertain both because CN/H_2 is uncertain and because our estimate of $N(CN)$ is based on LTE, which has most of the CN column density in states above $N = 1$. Moreover, $|\boldsymbol{B}|_{critical}$ is probably an overestimate of the expected $|\boldsymbol{B}|$ since the additional support provided by the observed supersonic motions is not included.

Our third method is to use the virial theorem. McKee et al. (1993) pointed out that complications due to internal density variations, surface pressure, and magnetic fields are generally ignored and introduced a virial parameter α to account for these complications. Then

$$M = \alpha^{-1}[5R\sigma^2/G] = 210\alpha^{-1} R\, \Delta V^2\ M_\odot\ , \quad (3)$$

with the cloud radius R in pc and the full-width at half-maximum line width ΔV in km s^{-1}. The expression in brackets is the usual one for a spherical cloud with uniform density and isotropic velocity dispersion σ. They argued that for the case in which "turbulent" motions and the magnetic field are of comparable importance in supporting a cloud and in which the cloud mass is twice the magnetic critical mass, the virial estimate with $\alpha \approx 1$ provides a reasonably accurate estimate of the mass. They also noted that under these conditions the mean field strength would be given by

$$|\boldsymbol{B}|_{virial} \approx 3\alpha^{-1}(5/G)^{1/2}\sigma^2/R \approx 15\alpha^{-1}\ \Delta V^2/R\ \mu G\ . \quad (4)$$

Their investigation of Mouschovias's (1976) models found that $1.1 \lesssim \alpha \lesssim 1.33$. Myers & Goodman (1988) considered a large sample of clouds for which observed radii, line widths, and masses were available; McKee et al. (1993) state that the Myers & Goodman results imply an average value $\alpha \approx 1.2$, with large scatter.

We estimated cloud masses M from equation (3) assuming $\alpha = 1.2$. Our results, M(OMC-N4) $\approx 10\ M_\odot$ and M(S106-CN) $\approx 22\ M_\odot$, are in excellent agreement with the virial mass of OMC-N4 from H_2CO observations ($M \approx 12\ M_\odot$, Wilson & Johnston 1989) and with the mass of S106-CN inferred from OH column density and cloud size observations ($M \approx 13\ M_\odot$, Roberts et al. 1995). With the assumption of uniform gas density and a spherical cloud, we may infer the volume density $n(H_2)_{virial}$ and column density $N(H_2)_{virial}$ of molecular hydrogen. Finally, we estimate $|\boldsymbol{B}|_{virial}$ from equation (4). We give the results of the virial analysis in Table 2.

The three methods of estimating the "expected" values of the magnetic field strengths in the two clouds are reasonably self-consistent. Our CN Zeeman observations do not detect the "expected" high field strengths. However, because of the spatial averaging over a telescope beam and a possible nonzero angle θ between the field and the line of sight, and with a sample of only two clouds, it is difficult to draw conclusions from this result. What is clear, however, is that CN Zeeman observations are capable of probing magnetic field in dense cloud cores, and that it is crucial to extend these observations to additional clouds, with higher sensitivity.

5. SUMMARY

We have carried out the first Zeeman observations in the 3 mm lines of CN toward two dense molecular cores, OMC-N4 and S106-CN. Both have H_2 volume densities of order 10^6 cm^{-3}. Estimates of the theoretically expected magnetic field strengths from the assumptions that (1) the observed line widths are sub-Alfvénic, (2) that mass to magnetic flux ratios are equal to the critical values, and (3) that the cores are in virial equilibrium all yield results that are several times higher than our limits on the line-of-sight component of the magnetic field. Either these theoretical assumptions are incorrect, or we are simply unlucky and the fields lie predominantly in the plane of the sky. Only Zeeman observations of additional cores can resolve this question.

We thank the staff at IRAM for construction of the polarimeter that made these observations possible, Gabriel Paubert for help with the observations, and Crystal Brogan for development of our least-squares fitting routine. R. M. C. and T. H. T. receive support from National Science Foundation grants AST9116917, AST9419227, and INT9116356.

REFERENCES

Bally, J., & Scoville, N. Z. 1982, ApJ, 255, 497
Batrla, W., Wilson, T. L., Bastien, P., & Ruf, K. 1983, A&A, 128, 279
Bel, N., & Leroy, B. 1989, A&A, 224, 206
Churchwell, E., & Bieging, J. H. 1982, ApJ, 258, 515
Crutcher, R. M., Churchwell, E., & Ziurys, L. M. 1984, ApJ, 283, 668
Crutcher, R. M. 1988, in Molecular Clouds in the Milky Way and External Galaxies, ed. R. Dickman, R. Snell, & J. Young (New York: Springer), 105
Crutcher, R. M., Troland, T. H., Goodman, A. A., Myers, P. C., Kazès, I., & Heiles, C. 1993, ApJ, 407, 175
Crutcher, R. M., Mouschovias, T.Ch., Troland, T. H., & Ciolek, G. E. 1994, ApJ, 427, 839
Gordy, W., & Cook, R. L. 1984, Microwave Molecular Spectra (3d ed.; New York: Wiley)
Graedel, T. E., Langer, W. D., & Frerking, M. A. 1982, ApJS, 48, 321

McKee, C. F., Zweibel, E., Goodman, A. A., & Heiles, C. 1993, in Protostars and Planets III, ed. E. H. Levy & J. I. Lunine (Tucson: Univ. Arizona Press), 327
Mouschovias, T. Ch. 1976, 207, 141
Mouschovias, T.Ch., & Spitzer, L. 1976, ApJ, 210, 326
Myers, P. C., & Goodman, A. A. 1988, ApJ, 329, 392
Roberts, D. A., Crutcher, R. M., & Troland, T. H. 1995, ApJ, 442, 208
Roberts, D. A., Crutcher, R. M., Troland, T. H., & Goss, W. M. 1993, ApJ, 412, 675
Troland, T. H. 1990, in IAU Symposium 140, Galactic and Extragalactic Magnetic Fields, ed. R. Beck, P. Kronberg, & R. Wielebinski (Dordrecht: Kluwer), p. 293
Troland, T. H., Crutcher, R. M., Goodman, A. A., Heiles, C., Kazès, I., & Myers, P. C. 1995, submitted to ApJ
Troland, T. H., Crutcher, R. M., & Kazès, I. 1986, ApJ, 304, L57
Troland, T. H., Heiles, C., & Goss, W. M. 1989, ApJ, 337, 342
Turner, B. E., & Thaddeus, P. 1977, ApJ, 211, 755
Wilson, T. L., & Johnston, K. J. 1989, ApJ, 340, 894